Supporting information

Distinguishing the nanoplastic–cell membrane interface by polymer type and aging properties: translocation, transformation and perturbation

Lingzhi Li,[ab] Shixin Li,[c] Yan Xu,[d] Luyao Ren,[b] Lin Yang,[b] Xia Liu,[b] Yanhui Dai,[b] Jian Zhao,[be] Tongtao Yue*[be]

[a] *College of Chemistry and Chemical Engineering, China University of Petroleum (East China), Qingdao 266580, China*

[b] *Institute of Coastal Environmental Pollution Control, Key Laboratory of Marine Environment and Ecology, Ministry of Education, Ocean University of China, Qingdao 266100, China. E-mail: yuetongtao@ouc.edu.cn*

[c] *Joint International Research Laboratory of Agriculture and Agri-product Safety of the Ministry of Education, Yangzhou University, Yangzhou 225009, China*

[d] *College of Electronic Engineering and Automation, Shandong University of Science and Technology, Qingdao 266590, China*

[e] *Laboratory of Marine Ecology and Environmental Science, Qingdao National Laboratory for Marine Science and Technology, Qingdao 266237, China*

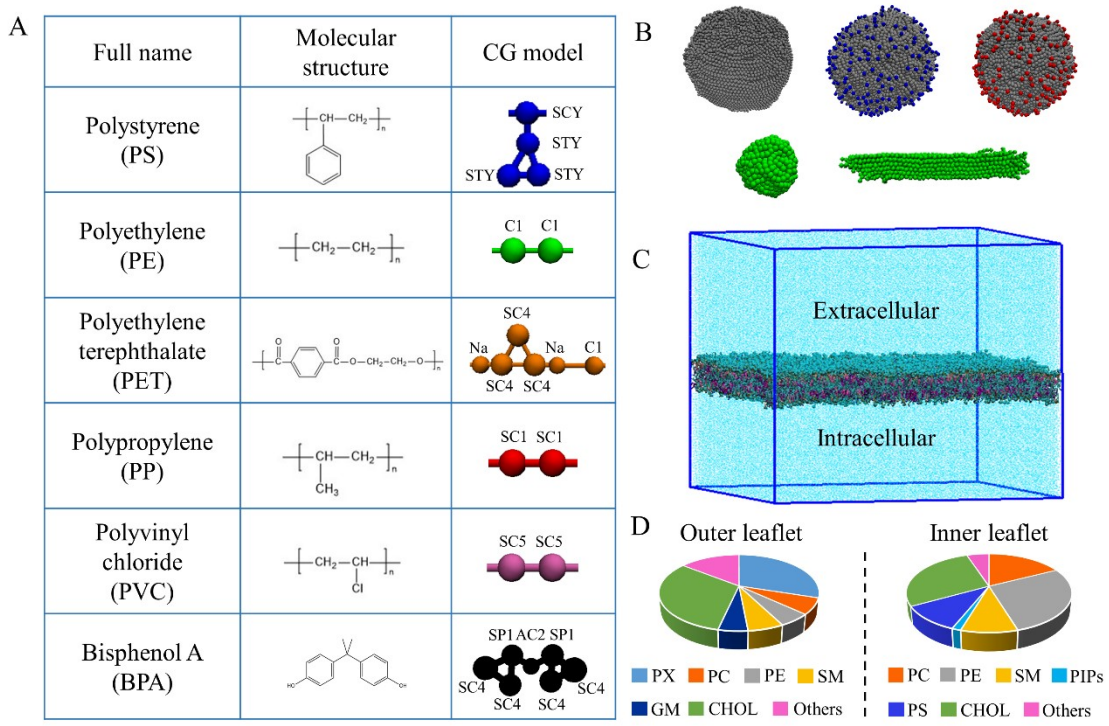

Fig. S1 Component models and simulation system setup. (A) Models of different polymers and BPA molecules used in simulations. (B) Representative structures of nanoplastics of different surface charges, sizes and shapes. Cationic and anionic groups on nanoplastic surfaces are shown as blue and red dots. Smaller and fiber-shaped nanoplastics are shown in green. (C) Multi-component mammalian cell membrane consisting of 63 different lipid species asymmetrically distributed across two leaflets. (D) Distributions of lipid species in two leaflets according to the tail length, saturation degree, and headgroup type.

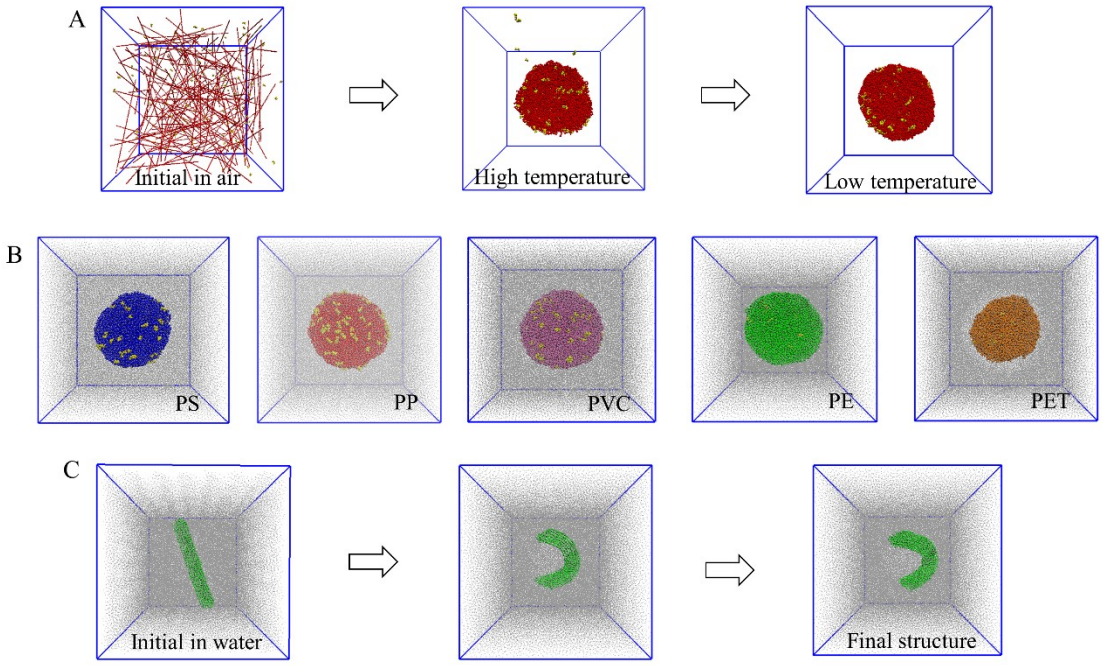

Fig. S2 Preparation of nanoplastics of different materials and properties. (A) The melting-annealing procedure to construct nanoplastics. Firstly, numerous polymers and BPA molecules self-aggregate in air at high temperature and the structure is further annealed and equilibrated at a lower temperature. (B) Equilibrium structures of nanoplastics of different polymer types in water. (C) Construction of the fiber-shaped PE nanoplastic. Polymers are initially positioned closely in parallel, and equilibrated in water.

Table S1. Melting (T_m) and glass transition (T_g) temperatures for plastics of five polymer types considered in our simulations.

Polymer type	PS	PE	PET	PP	PVC
T_m (°C)	250 - 290	180 - 270	260-280	200 - 280	160-210
T_g (°C)	90	-110	73-78	-20	-50 - -5

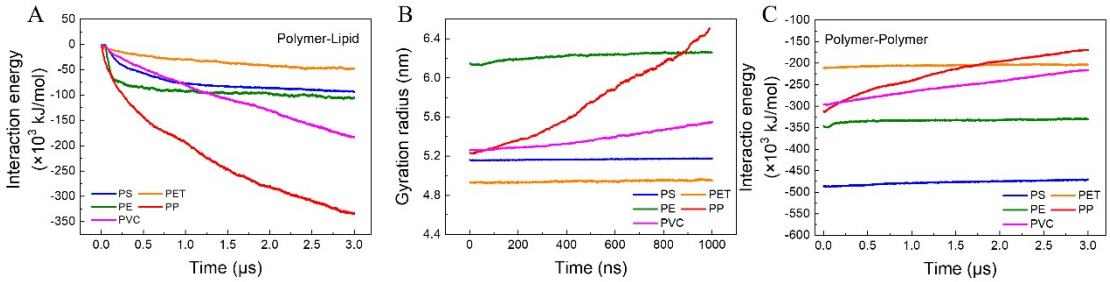

Fig. S3 Characterization of cell membrane interactions with nanoplastics of different polymer types. (A) Time evolutions of the polymer-lipid interaction energy. (B) Time evolutions of the gyration radius of different nanoplastics during their interactions with membrane. (C) Time evolutions of the polymer-polymer interaction energy.

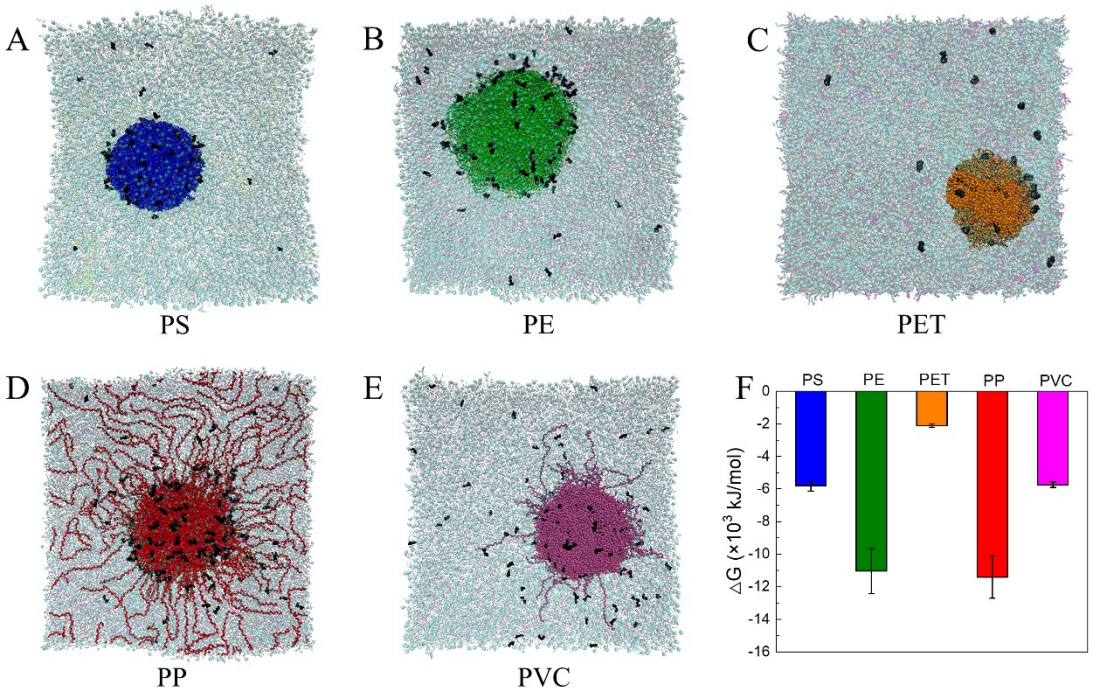

Fig. S4 Leakage of BPA molecules from nanoplastics due to nanoplastic-cell membrane interactions. (A-E) Top views of the nanoplastic-cell membrane interactions with BPA molecules colored in black. Lipids are set semi-transparent for viewing released BPA molecules. (F) Change of the interaction energy between BPA molecules and lipids for comparing the extent of BPA leakage from nanoplastics of different polymer types. The highest extent of BPA leakage from PP nanoplastic is ascribed to its dissolution, while the high value for PE nanoplastic is primarily due to shallower initial distribution of BPAs in nanoplastic.

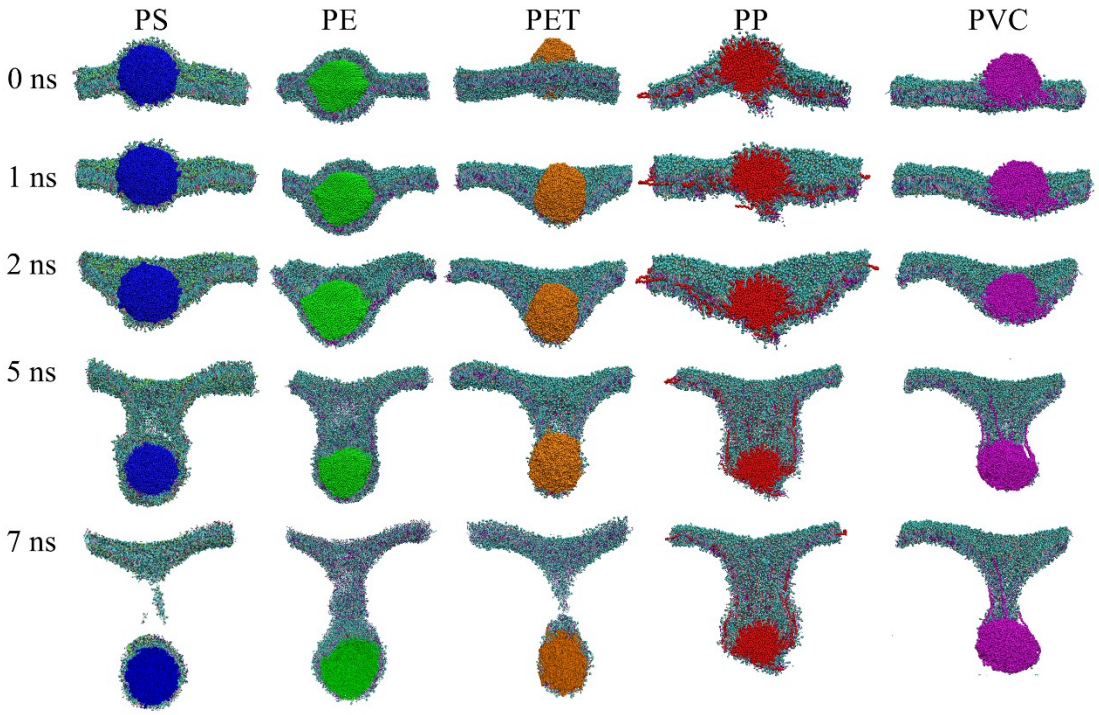

Fig. S5 Cross-sectional views of snapshots at different time points depicting mechanical translocation of different nanoplastics through the membrane.

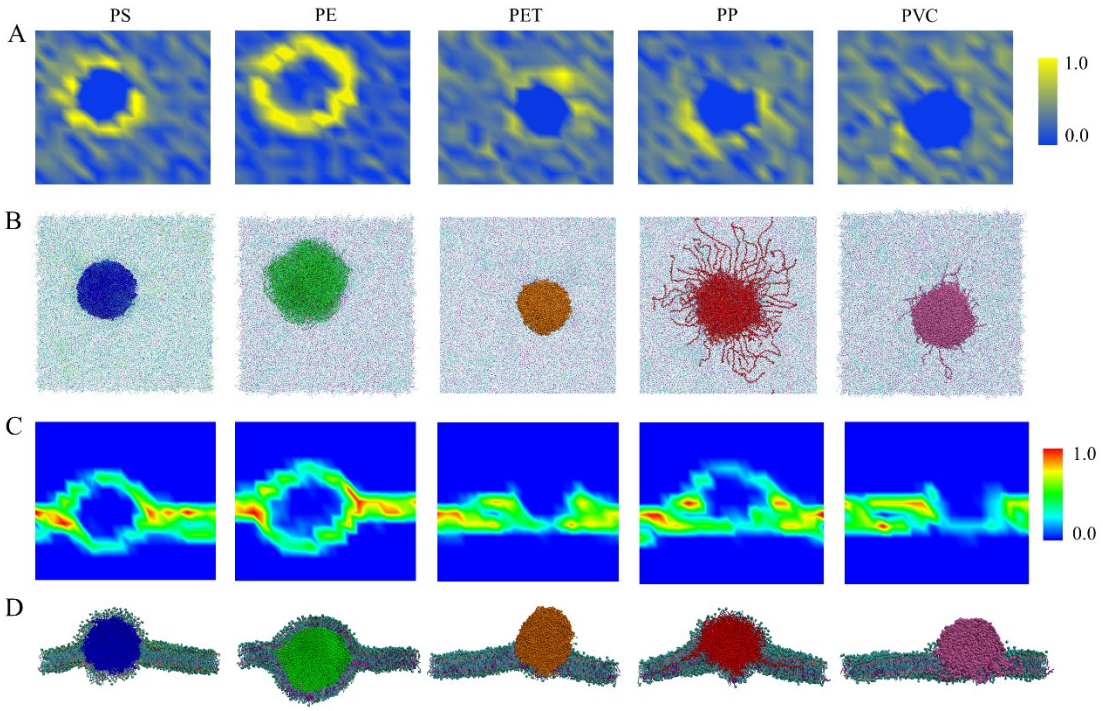

Fig. S6 Membrane perturbation induced by nanoplastics. (A) Lateral lipid density distribution after membrane interactions with different nanoplastics. (B) Top views of the final snapshots. (C) Local lipid density distributions from the cross-sectional view. (D) Cross-sectional views of the final simulated snapshots.

Table S2 Dynamic and mechanical properties of membranes influenced by nanoplastics of different polymer types. [a]

Properties / System	Diffusion coefficient D_L (10^{-7} cm^2/s)	Area compressibility modules K_A (mN/m)	Bending modules K_B (k_B/T)
Pure membrane	1.87	367.09	21.88
Membrane + PS	1.45	213.93	12.75
Membrane + PE	1.74	232.49	18.02
Membrane + PET	1.72	238.32	14.21
Membrane + PP	1.42	201.04	11.99
Membrane + PVC	1.59	211.78	12.63

[a] D_L indicates the average diffusion coefficient of all membrane components, K_A is the area compressibility modulus, and K_B is the bending modulus.

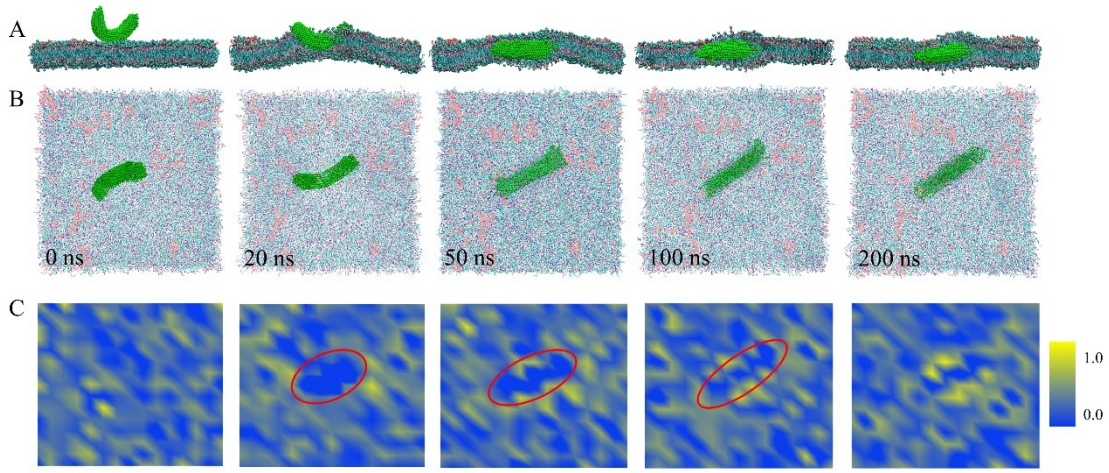

Fig. S7 Spontaneous translocation of a fiber-shaped nanoplastic into the membrane. (A, B) Cross-sectional (A) and top (B) views of typical snapshots depicting membrane translocation of the fiber-shaped nanoplastic. (C) Top views of the lipid density distribution at different time points. Locations of the fiber-shaped nanoplastic are labeled with red circles for illustrating the transient membrane perturbation.

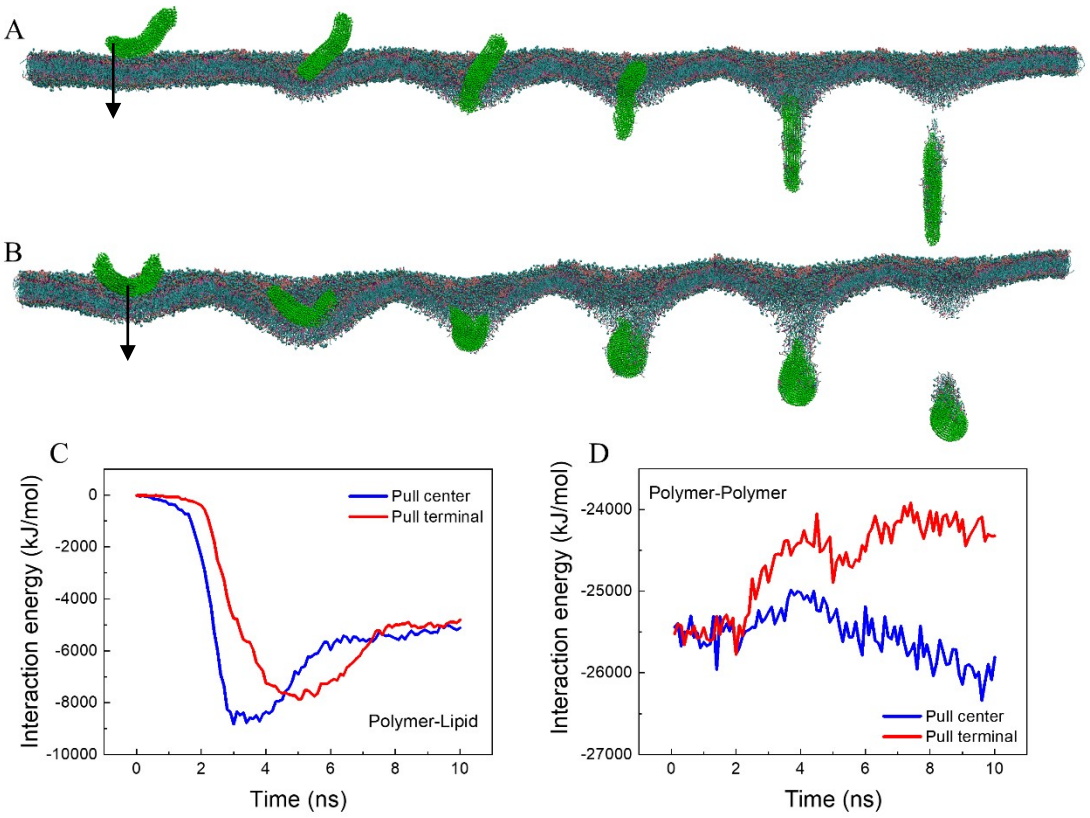

Fig. S8 Mechanical translocation of a fiber-shaped nanoplastic through the membrane. (A, B) Time sequences of typical snapshots depicting two modes of fiber-shaped nanoplastic translocation through the membrane. To accomplish translocation, an external force of spring constant 2000 kJ/mol/nm^2 was applied on the nanoplastc tip (A) or center (B) to pull it along the membrane normal direction at a constant velocity of 0.001 nm/ps. (C, D) Time evolutions of the polymer-lipid (C) and polymer-polymer (D) interaction energies during nanoplastic translocation through the membrane in two pathways.

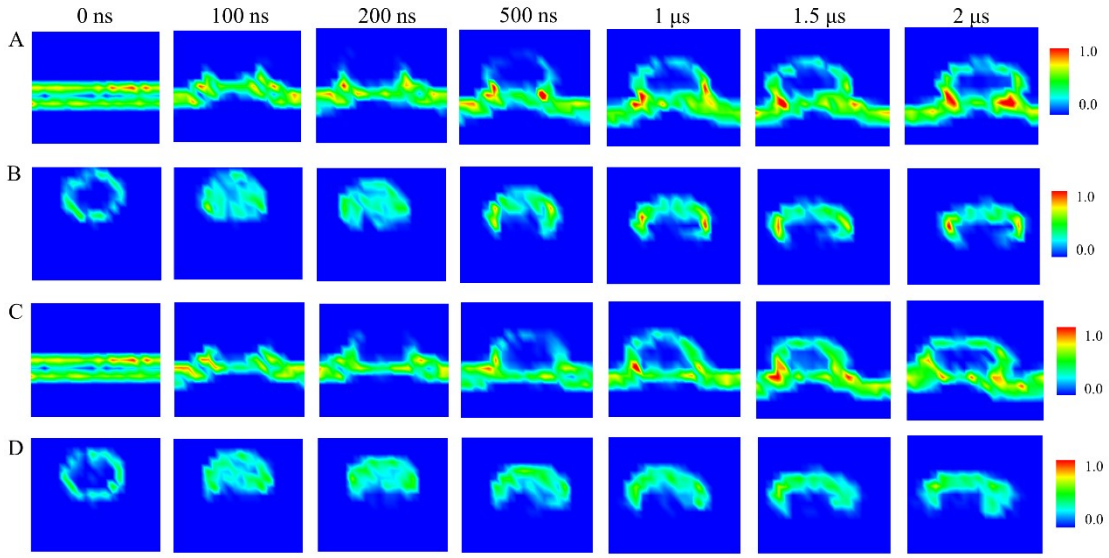

Fig. S9 Lipid and surface charge rearrangement at cell membrane interfaces with anionic (A, B) and cationic (C, D) nanoplastics. (A, C) Cross-sectional views of the lipid density distribution induced by the anionic (A) and cationic (C) nanoplastics at different time points. (B, D) Density distributions of charged groups on the anionic (B) and cationic (D) nanoplastics during their interactions with membrane.

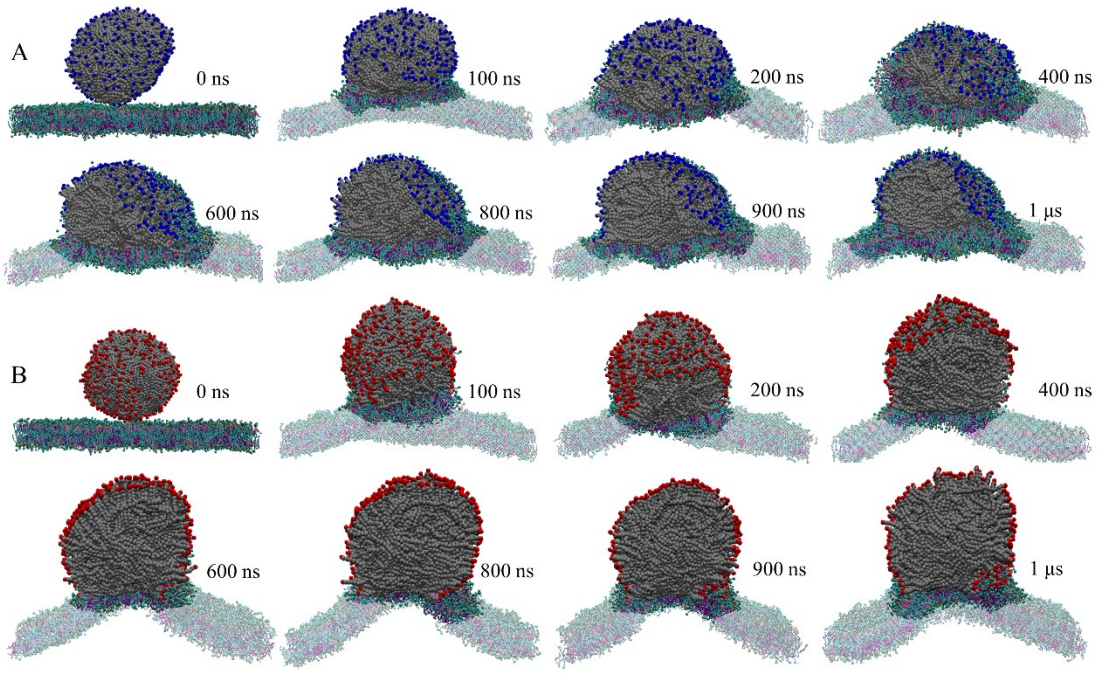

Fig. S10 Cross sectional views of the simulated snapshots at different time points illustrating cell membrane interactions with the cationic (A) and anionic (B) nanoplastics. Lipids not in contact with the nanoplastics are set semi-transparent for illustrating the rearrangement of lipids around nanoplastics.

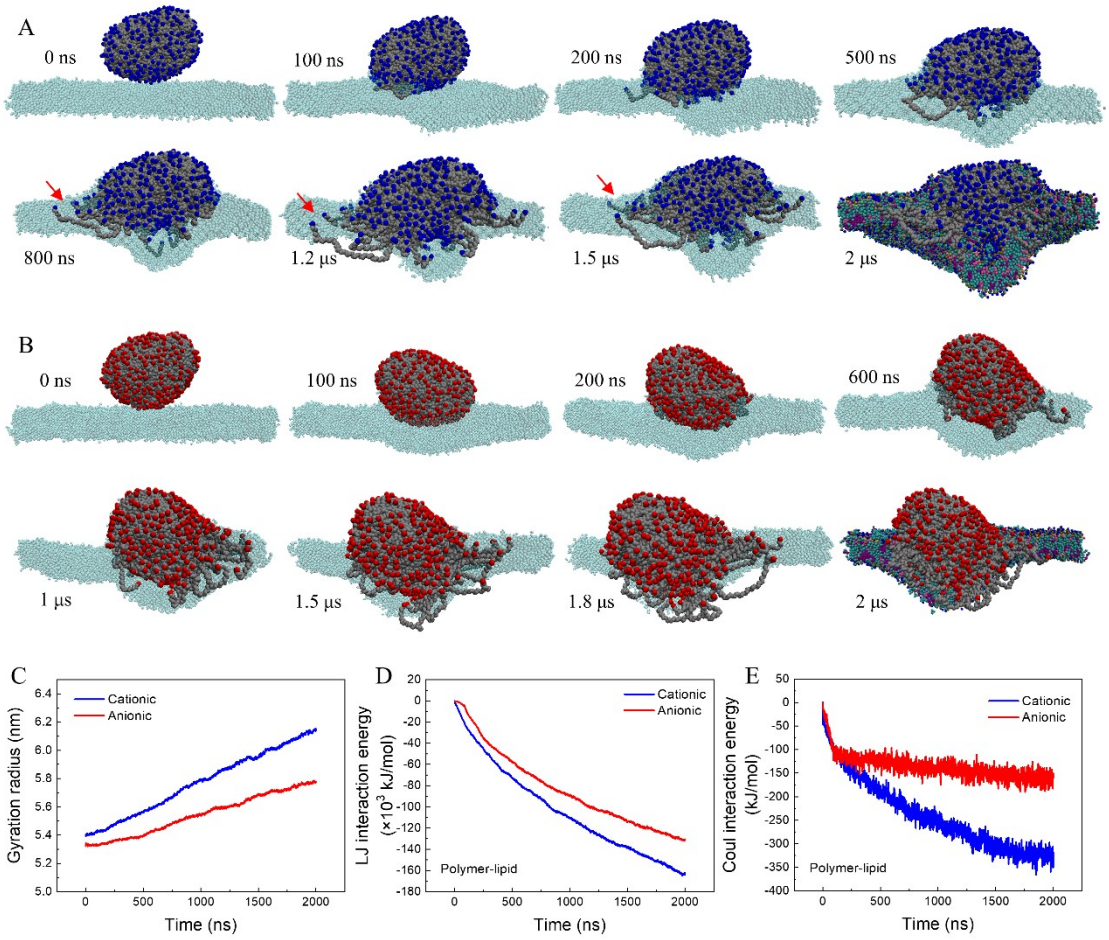

Fig. S11 Surface charge effect on PP nanoplastic interactions with cell membrane. (A, B) Time sequence of typical snapshots depicting cationic (A) and anionic (B) PP nanoplastic interactions with membrane. Red arrows denote protruson of several polymers with terminal cationic groups getting in contact with negatively charged lipid headgroups. (C) Gyration radius of cationic and anionic nanoplastics during cell membrane interactions. (D, E) Time evolutions of the van der Waals (D) and electrostatic (E) interaction energies between differently charged nanoplastics and lipids.